

**Copper hexacyanoferrate nanoparticles as cathode material
for aqueous Al-ion batteries**

Journal:	<i>Journal of Materials Chemistry A</i>
Manuscript ID:	TA-COM-09-2014-004644.R1
Article Type:	Communication
Date Submitted by the Author:	29-Oct-2014
Complete List of Authors:	Liu, Sheng; Nankai University, Inst. of New Energy Material Chemistry Pan, Guiling; Nankai University, Inst. of New Energy Material Chemistry Li, Guoran; Nankai University, Inst. of New Energy Material Chemistry Gao, Xueping; Nankai University, Inst. of New Energy Material Chemistry

Copper hexacyanoferrate nanoparticles as cathode material for aqueous Al-ion batteries

Cite this: DOI: 10.1039/x0xx00000x

S. Liu, G. L. Pan, G. R. Li and X. P. Gao*

Received XXth XXXXXXXX 20XX,
Accepted XXth XXXXXXXX 20XX

DOI: 10.1039/c000000x

www.rsc.org/MaterialsA

Copper hexacyanoferrate (CuHCF) nanoparticles with Prussian blue structure are prepared via a simple co-precipitation method, which present the ability to insert Al ions reversibly in aqueous solution. CuHCF is verified to be a promising cathode material for aqueous Al-ion batteries.

Lithium-ion batteries (LIBs) with organic electrolytes have become the most widely adopted power sources for portable electronics. It is predicted that the growing electric vehicle market will lead to a skyrocketing demand for LIBs in the near future.^{1–3} However, the concerns on lithium resource reservation and geographical distribution have driven researchers to search for alternatives to Li battery system.⁴ Nowadays, emerging sodium ion batteries have attracted much attention due to the low cost and wide availability of sodium.^{5–7} The common feature of the Li-ion or Na-ion batteries is that the same monovalent ions (Li^+ or Na^+) can be reversibly inserted and extracted into/from the electrode materials with a simultaneous charge-transfer in host materials, and the host structure can be readily maintained. Thus, the insertion/extraction reaction with such monovalent ions promises a prolonged lifetime for the electrode active materials.² If a guest ion can carry two or three charges, the insertion reaction would store more energy than that in Li-ion or Na-ion batteries.⁸ A key issue toward multivalent ion insertion is the ion mobility in host materials, which is highly dependent on the size and charge of the guest ion. Large and multivalent ions could easily fall into a combined energetic/steric trap and block the ion mobility.⁹ Divalent ion batteries, such as Zn-ion and Mg-ion batteries, have been proposed and studied intensively in recent years.^{10–13} Especially, investigation on Mg^{2+} insertion in host materials has made fast progress. However, exploring host materials to improve Mg^{2+} transport kinetics for Mg-ion batteries remains a major challenge.^{9,14}

Recently, trivalent aluminum ions have been proposed to reversibly insert into some host materials, such as V_2O_5 , VO_2 and TiO_2 .^{8,15–17} Our previous work has revealed that the TiO_2 nanotube arrays could insert Al ions in aqueous solution, which could be used as anode material for aqueous Al-ion batteries.¹⁷ Success with Al ion insertion into TiO_2 has motivated us to explore new cathode materials for aqueous Al-ion batteries. Vanadium oxides seem to be available option, however, the toxicity of vanadium oxides makes these compounds apart from the consideration in future application. Due to the slow diffusion kinetics mainly caused by the strong

bonding between Al ions and host structure, the choice for host materials is limited to a great extent. Based on structure analysis, Prussian blue analogues (PBAs) may be a kind of potential materials for Al ion insertion. Here, PBAs can be rewritten as a general formula $\text{A}_x\text{PR}(\text{CN})_6$. P and R ions are separated and bonded by CN ligands to form a face-centred cubic structure with open framework, which contains large interstitial A sites for introducing guest ions or molecules. The electrochemical properties of PBAs have been intensively studied as hydrogen storage, battery electrodes and electrochromic materials for decades.^{18–22} Recently, the nickel hexacyanoferrate and copper hexacyanoferrate with Prussian blue structure are demonstrated to electrochemically insert ions in aqueous solutions.²³ These ions could be monovalent ions (Li^+ , Na^+ , K^+ and NH_4^+) and divalent ions (Mg^{2+} , Ca^{2+} , Sr^{2+} and Ba^{2+}).^{24–28} As electrode materials, PBAs present good electrochemical performance with high-rate capability and long cycle life. Furthermore, these compounds can be synthesized by a simple co-precipitation method, which is easily scaled up for large-scale energy storage application.

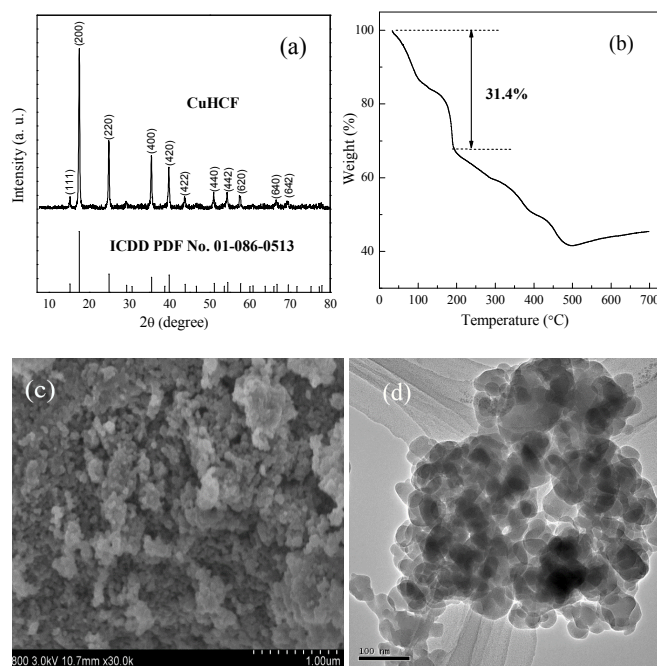


Fig. 1 XRD pattern (a), TG curve (b), SEM image (c) and TEM image (d) of the as-prepared CuHCF powders.

Although, the monovalent and divalent cations are facile to insert into PBAs framework, the insertion reaction of trivalent cations would carry more charges into PBAs. In this communication, trivalent aluminium ion storage of copper hexacyanoferrate (CuHCF) as cathode material for aqueous Al-ion battery is investigated for the first time.

CuHCF nanoparticles are prepared by a simple co-precipitation method as reported previously (see ESI).^{24,27,29} The XRD pattern of the as-prepared sample is shown in Fig. 1a. The as-prepared CuHCF powders show high crystallinity degree and all the reflections are indexed as the face-centered cubic Prussian blue structure (ICDD PDF card No.01-086-0513). The lattice parameter of the CuHCF is calculated to be 10.16 Å, and the average crystallite size is 33 nm derived from XRD data. The open framework and nanocrystallites of CuHCF make it possible to insert large hydrated cations reversibly.

As the valences of Fe and Cu in CuHCF are +3 and +2, respectively, the molecular formula of the as-prepared CuHCF powders could be written as $\text{KCu}[\text{Fe}(\text{CN})_6] \cdot x\text{H}_2\text{O}$, in which the value of x represents the amount of zeolitic water residing in the cavities of CuHCF. To determine the x value, TG test has been conducted under Ar atmosphere and the result is shown in Fig. 1b. The weight loss before 200 °C is derived from zeolitic water, and the content of zeolitic water is deduced to be 31.4%. Based on the weight loss, the x value is calculated to be 8, thus the molecular formula of the as-prepared CuHCF material can be rewritten as $\text{KCu}[\text{Fe}(\text{CN})_6] \cdot 8\text{H}_2\text{O}$. It is noted here that the content of zeolitic water in CuHCF is related to the temperature and moisture of the environment, so the accurate molecule weight is hardly definite. The residual zeolitic water within the framework can play the role of shielding on the charge of multi-valent ions and facilitates ion insertion.³⁰ This behaviour mentioned above has also been illustrated by V_2O_5 cathode in Mg ion batteries, the zeolitic water in V_2O_5 can shield the charge of Mg^{2+} ion and improve the diffusion kinetics to a great extent.^{14,31} Al^{3+} ion has a small ionic radius of 39 pm and a high valence of +3, it is easy to fall into an energetic trap in host materials and block the ion mobility. The zeolitic water in CuHCF is believed to help shield the charge of Al^{3+} ion and reduce its electrostatic forces with host structure, thus enhanced diffusion kinetics is expected.

The CuHCF nanoparticles are uniformly distributed as indicated in Fig. 1c. The particle size is around 30-50 nm as shown in TEM image (Fig. 1d), slightly larger than that in XRD analysis due to the aggregation of nano-crystallites. The small particle size could reduce diffusion distances of guest ions transporting in the solid phases, thus enhanced high-rate performance is feasible towards the battery applications. It is worth highlighting that the present method to prepare nano-sized CuHCF is facile and easily scaled up, which is significant in large-scale energy storage application by virtue of low cost.

Fig. 2 shows cyclic voltammogram (CV) of CuHCF electrode in 0.5 M $\text{Al}_2(\text{SO}_4)_3$ aqueous solution at the scan rate of 1 mV s^{-1} . The broad peaks are observed over a wide potential range between 0.2 and 1.2 V (vs. SCE). The anodic peaks are located at 0.79 V and 0.85 V (vs. SCE), and two cathodic peaks are centered at 0.81 V and 0.53 V (vs. SCE). It means that the two-step reactions happen in the

Al^{3+} ion insertion/extraction process in CuHCF. The result is different from the behavior of monovalent ions (Na^+ and K^+) in PBAs as reported previously.^{25–27} However, a similar result can be observed on the insertion reaction of divalent ions (Mg^{2+} , Ca^{2+} and Sr^{2+}) in PBAs.²⁸ It is suggested from the relationship between hydration energy and the insertion potential of guest ions that there is a dehydration reaction process during divalent ion insertion.^{28,32} This unique behavior here is attributed to the steric effect of hydrated Al^{3+} ions when inserting into CuHCF framework. Theoretically, Al^{3+} ion has a smaller Shannon radius (39 pm) as compared with Li^+ ion (59 pm), Na^+ ion (102 pm), K^+ ion (151 pm) and Mg^{2+} ion (72 pm). However, the hydrated Al^{3+} ion is larger with a radius of 4.8 Å, while the channels connecting the sites of guest ions are only about 1.6 Å in size.²⁷ Therefore, the desolvation process of hydrated Al^{3+} ions is necessary before the insertion and diffusion process in the bulk. Moreover, different anions could affect the state of hydrated Al^{3+} ions in the aqueous solution, leading to the slight shift of the anodic/cathodic peaks in Cl^- and NO_3^- containing solution (see Fig S1). At the same time, as the partly hydrated ions diffusing in the skeletal structure, the interchange of nearby water and the rotation of the hydration sheaths of Al^{3+} ions may be existed, similar to the Li^+ ion in lithium sulfates.²⁷ It is demonstrated from the wide anodic/cathodic peaks in CV curve that the Al^{3+} ion mobility in CuHCF framework is limited due to the strong bonding between Al^{3+} ions and CN ligands. Still, the insertion chemistry of Al^{3+} ions in CuHCF is realized, because the residual zeolitic water can shield charge concentration effectively. After insertion into CuHCF framework, Al^{3+} or hydrated Al^{3+} ions reside in the A site as illustrated in the schematic diagram in Fig. 2. It is noted here that the available A sites are only partly occupied by Al^{3+} or partly-hydrated Al^{3+} ions to retain the charge neutrality in the oxidized state of CuHCF.

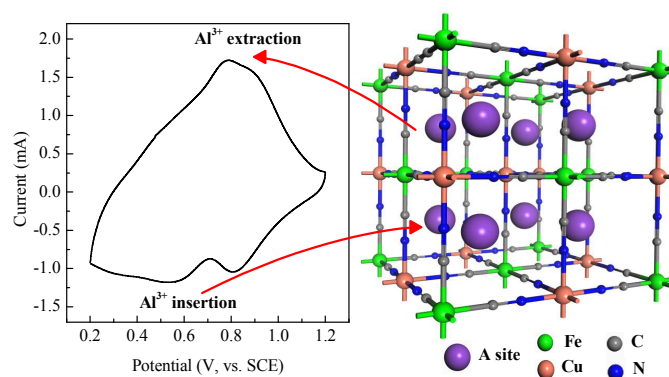


Fig. 2 Typical CV curve of the CuHCF electrode in aqueous $\text{Al}_2(\text{SO}_4)_3$ and the schematic positions of Al^{3+} in CuHCF framework.

To evaluate the electrochemical performance of CuHCF in Al^{3+} ions in aqueous solution, the three-electrode cell is fabricated. The typical charge and discharge curves at different current densities are shown in Fig. 3a. The discharge curves show potential slope over a wide potential range. Two sloping discharge plateaus are observed in the discharge process, corresponding to the two cathodic peaks in the CV curve. In the discharge process, Al^{3+} ions insert into CuHCF structure, and partly occupy the tetrahedrally coordinated A sites, which are contained in nitrogen-coordinated Cu^{2+} ions and hexacyanoferrate (III) complexes ($\text{Fe}(\text{CN})_6$) to form face-centered cubic open framework as indicated in Fig. 2.^{27,28} At the same time,

the carbon-coordinated Fe^{3+} ions are reduced to Fe^{2+} , while nitrogen-coordinated Cu^{2+} ions keep electrochemically inactive, but rather contribute only to maintain the stable framework.³³ To further analyze the structure of the Al^{3+} inserted CuHCF, XRD measurement is performed. However, there is no evident change as compared to that of the pristine electrode, demonstrating that the framework of CuHCF could be maintained in the Al^{3+} ion insertion/extraction process (Fig. S2).

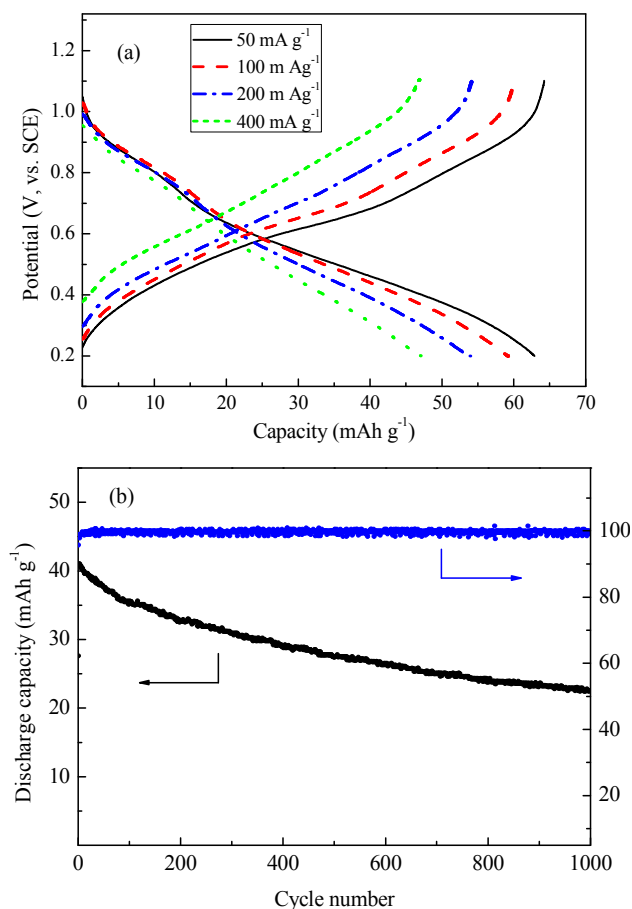


Fig. 3 Charge/discharge curves at different current densities (a) and cycle performance at the current density of 400 mA g^{-1} of the CuHCF electrode (b) in $0.5 \text{ M Al}_2(\text{SO}_4)_3$ aqueous solution.

Although the accurate molecular weight of CuHCF is affected by the environmental humidity and temperature, the theoretical capacity of CuHCF can still be estimated to be 58.9 mAh g^{-1} based on the molecular formula of $\text{KCu}[\text{Fe}(\text{CN})_6] \cdot 8\text{H}_2\text{O}$ and the redox couple of $\text{Fe}^{3+}/\text{Fe}^{2+}$. A specific capacity of 62.9 mAh g^{-1} is obtained at the current density of 50 mA g^{-1} , which is reasonable and close to the value in the electrolyte containing Na^+ , K^+ , and NH_4^+ ions as reported elsewhere.²⁷ It means that the specific capacity is highly depended on the $\text{Fe}^{3+}/\text{Fe}^{2+}$ redox couple in the framework of CuHCF rather than the guest species. However, the kinetic properties of the CuHCF are mainly related to the species and charge numbers of the guest ions as discussed above. The discharge mid-potential is 0.54 V (vs. SCE), making CuHCF appropriate as cathode materials for aqueous aluminum ion battery. The high-rate capability of CuHCF also performs outstanding. To evaluate the high-rate capability, different current densities are conducted to charge and discharge the

CuHCF electrode. The discharge capacity of 46.9 mAh g^{-1} is obtained at 400 mA g^{-1} with retention of 74.6% towards the capacity at 50 mA g^{-1} . Though the kinetics is limited, the nano-crystallites and residual water in the framework of CuHCF are helpful to shorten the diffusion path and increase diffusion kinetics of Al^{3+} ions, thus the enhanced rate capability is obtained.

Cycle performance test is conducted at the current density of 400 mA g^{-1} . The maximum discharge capacity reaches 41.0 mAh g^{-1} at the second cycle. Then, the capacity is gradually decreased to 22.5 mAh g^{-1} after 1000 cycles with retention of 54.9%. In particular, the coulombic efficiency keeps about 100% during long cycling, indicating the high utilization and low side reactions of CuHCF in aqueous solutions. The capacity loss may be due to the dissolution of CuHCF in the acidic aqueous $\text{Al}_2(\text{SO}_4)_3$ solution. The issue of capacity decay of CuHCF should be addressed and conquered in the future work for a long stability.

The electrochemical capacity is intrinsically low in the case of CuHCF owing to the limitation of the theoretical capacity. However, CuHCF is still promising in large-scale energy storage applications in virtue of the low cost, environmental friendliness and safety by using simple synthesis method and aqueous electrolyte. More importantly, the successful reversible insertion of aluminum ions into host structure opens a door to multivalent insertion chemistry, which may increase energy density to a great extent by employing the light-weight host materials with multi-electron reaction.

In summary, copper hexacyanoferrate (CuHCF) nanoparticles are prepared by a simple and scalable co-precipitation method. The as-prepared CuHCF nanoparticles show the ability to insert aluminum ion reversibly in aqueous solution, making it a potential cathode material for aqueous Al ion batteries. Most importantly, the exploration of multivalent ion insertion/extraction reactions may provide alternatives to current lithium ion battery system for energy conversion and storage.

Acknowledgements

Financial Supports from the 973 Program (2015CB251100), NFSC (21421001), and MOE Innovation Team (IRT13022) of China are gratefully acknowledged.

Notes and references

Institute of New Energy Material Chemistry, Collaborative Innovation Center of Chemical Science and Engineering (Tianjin), Tianjin Key Laboratory of Metal and Molecule Based Material Chemistry, Nankai University, Tianjin 300071, China. Fax: +86-22-23500876; Tel: +86-22-23500876; E-mail: xpgao@nankai.edu.cn

† Electronic Supplementary Information (ESI) available: Experimental details. See DOI: 10.1039/c000000x/

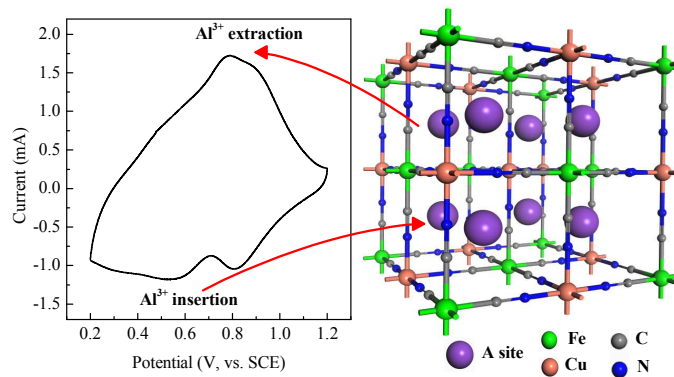
- Z. G. Yang, J. L. Zhang, M. C. W. Kintner-Meyer, X. C. Lu, D. W. Choi, J. P. Lemmon and J. Liu, *Chem. Rev.*, 2011, **111**, 3577.
- M. Armand and J. M. Tarascon, *Nature*, 2008, **451**, 652.
- X. P. Gao and H. X. Yang, *Energy Environ. Sci.*, 2010, **3**, 174.
- D. Slater, D. Kim, E. Lee and C. S. Johnson, *Adv. Funct. Mater.*, 2013, **23**, 947.
- J. F. Qian, M. Zhou, Y. L. Cao, X. P. Ai and H. X. Yang, *Adv. Energy Mater.*, 2012, **2**, 410.

6. D. W. Su, S. X. Dou and G. X. Wang, *J. Mater. Chem. A*, 2014, **2**, 11185.
7. Y. Fang, L. F. Xiao, J. F. Qian, X. P. Ai, H. X. Yang and Y. L. Cao, *Nano lett.*, 2014, **14**, 3539.
8. W. Wang, B. Jiang, W. Y. Xiong, H. Sun, Z. H. Lin, L. W. Hu, J. G. Tu, J. Hou, H. M. Zhu and S. Q. Jiao, *Sci. Rep.*, 2013, **3**, 3383.
9. E. Levi, G. Gershinsky, D. Aurbach, O. Isnard and G. Ceder, *Chem. Mater.*, 2009, **21**, 1390.
10. C. J. Xu, B. H. Li, H. D. Du and F. Y. Kang, *Angew. Chem. Int. Edit.*, 2012, **124**, 957.
11. M. G. Kim and J. Cho, *Adv. Funct. Mater.*, 2009, **19**, 1497.
12. B. Liu, T. Luo, G. Y. Mu, X. F. Wang, D. Chen and G. Z. Shen, *ACS Nano*, 2013, **7**, 8051.
13. Y. Y. Shao, G. Meng, X. L. Li, Z. M. Nie, P. J. Zuo, G. S. Li, T. B. Liu, J. Xiao, Y. W. Cheng, C. M. Wang, J. G. Zhang and J. Liu, *Nano lett.*, 2013, **14**, 255.
14. E. Levi, Y. Gofer and D. Aurbach, *Chem. Mater.*, 2009, **22**, 860.
15. N. Jayaprakash, S. Das and L. Archer, *Chem. Commun.*, 2011, **47**, 12610.
16. Y. J. He, J. F. Peng, W. Chu, Y. Z. Li and D. G. Tong, *J. Mater. Chem. A*, 2014, **2**, 1721.
17. S. Liu, J. J. Hu, N. F. Yan, G. L. Pan, G. R. Li and X. P. Gao, *Energy Environ. Sci.*, 2012, **5**, 9743.
18. V. D. Neff, *J. Electrochem. Soc.*, 1978, **125**, 886.
19. K. Itaya, I. Uchida and V. D. Neff, *Accounts Chem. Res.*, 1986, **19**, 162.
20. D. Stilwell, K. Park and M. Miles, *J. Appl. Electrochem.*, 1992, **22**, 325.
21. N. R. de Tacconi, K. Rajeshwar and R. O. Lezna, *Chem. Mater.*, 2003, **15**, 3046.
22. N. L. Rosi, J. Eckert, M. Eddaoudi, D. T. Vodak, J. Kim, M. O'Keeffe and O. M. Yaghi, *Science*, 2003, **300**, 1127.
23. Z. Chang, Y. Q. Yang, M. X. Li, X. W. Wang and Y. P. Wu, *J. Mater. Chem. A*, 2014, **2**, 10739.
24. C. D. Wessells, R. A. Huggins and Y. Cui, *Nat. Commun.*, 2011, **2**, 550.
25. C. D. Wessells, S. V. Peddada, R. A. Huggins and Y. Cui, *Nano Lett.*, 2011, **11**, 5421.
26. M. Pasta, C. D. Wessells, R. A. Huggins and Y. Cui, *Nat. Commun.*, 2012, **3**, 1149.
27. C. D. Wessells, S. V. Peddada, M. T. McDowell, R. A. Huggins and Y. Cui, *J. Electrochem. Soc.*, 2012, **159**, A98.
28. R. Y. Wang, C. D. Wessells, R. A. Huggins and Y. Cui, *Nano Lett.*, 2013, **13**, 5748.
29. C. D. Wessells, M. T. McDowell, S. V. Peddada, M. Pasta, R. A. Huggins and Y. Cui, *ACS nano*, 2012, **6**, 1688.
30. H. Lee, Y. I. Kim, J. K. Park and J. W. Choi, *Chem. Commun.*, 2012, **48**, 8416.
31. P. Novak, W. Scheifele, F. Joho and O. Haas, *J. Electrochem. Soc.*, 1995, **142**, 2544.
32. F. Scholz and A. Dostal, *Angew. Chem. Int. Edit.*, 1996, **34**, 2685.
33. Z. J. Jia, J. Wang and Y. Wang, *RSC Adv.*, 2014, **4**, 22768.

Copper hexacyanoferrate nanoparticles as cathode material for aqueous aluminum ion batteries

S. Liu, G. L. Pan, G. R. Li, X. P. Gao

TOC



Copper hexacyanoferrate (CuHCF) nanoparticles with Prussian blue structure present the ability to insert Al ions reversibly in aqueous solution.